

THESIS FOR THE DEGREE OF  
LICENTIATE OF PHILOSOPHY

**SYNCHROTRON RADIATION  
FROM RUNAWAY ELECTRONS  
IN PLASMAS**

Adam Stahl



**CHALMERS**  
UNIVERSITY OF TECHNOLOGY

Department of Applied Physics  
Chalmers University of Technology  
Göteborg, Sweden, 2015

SYNCHROTRON RADIATION FROM RUNAWAY ELECTRONS IN PLASMAS  
Adam Stahl

© Adam Stahl, 2015

Technical Report No. CTH-NT-308  
ISSN 1653-4662  
Nuclear Engineering  
Department of Applied Physics  
Chalmers University of Technology  
SE-412 96 Göteborg  
Sweden  
Telephone +46-(0)31-772 10 00

Printed in Sweden by  
Reproservice  
Chalmers Tekniska Högskola  
Göteborg, Sweden, 2015

Adam Stahl  
Department of Applied Physics  
Chalmers University of Technology

## Abstract

Highly relativistic runaway electrons are of great concern in the area of fusion energy research, since their presence in tokamak plasmas have the potential to hinder the successful and stable operation of the device, and potentially cause severe structural damage. In this thesis, runaway electron generation dynamics is investigated using the newly developed efficient computational tool CODE. A particular emphasis is given to the synchrotron radiation emitted by the runaways, as this is an important source of information about their properties. The synchrotron emission spectrum is studied, as well as the effects of radiation back-reaction on the electron distribution and the runaway electron dynamics.

Synchrotron emission back-reaction is found to have a significant impact on the runaway distribution, leading to an increase in the critical electric field for runaway generation, as well as the appearance of non-monotonic features in the runaway tail for electric-field strengths above a certain threshold, potentially acting as a source of bump-on-tail instabilities. Both of these effects may contribute to reduce the severity of the runaway problem, although their importance is largest at high temperatures and low densities, likely making the impact in a tokamak disruption scenario limited. It is also found that the previously used approximation of considering only the emission from the most strongly emitting particles when modeling the synchrotron spectrum from runaway distributions can produce highly inaccurate results, and that the use of the full runaway distribution in this context is necessary.

**Keywords:** runaway electrons, synchrotron radiation, critical electric field, fusion plasma physics, tokamak



# Publications

- A** M. Landreman, A. Stahl, and T. Fülöp,  
*Numerical calculation of the runaway electron distribution function and associated synchrotron emission*,  
Computer Physics Communications **185**, 847-855 (2014).  
<http://dx.doi.org/10.1016/j.cpc.2013.12.004>  
<http://arxiv.org/abs/1305.3518>
- B** A. Stahl, E. Hirvijoki, J. Decker, O. Embréus, and T. Fülöp,  
*Effective critical electric field for runaway electron generation*.  
Accepted for publication in Physical Review Letters.  
<http://arxiv.org/abs/1412.4608>
- C** E. Hirvijoki, I. Pusztai, J. Decker, O. Embréus, A. Stahl and T. Fülöp,  
*Radiation reaction induced non-monotonic features in runaway electron distributions*.  
Submitted to Journal of Plasma Physics.  
<http://arxiv.org/abs/1502.03333>
- D** A. Stahl, M. Landreman, G. Papp, E. Hollmann, and T. Fülöp,  
*Synchrotron radiation from a runaway electron distribution in tokamaks*,  
Physics of Plasmas **20**, 093302 (2013).  
<http://dx.doi.org/10.1063/1.4821823>  
<http://arxiv.org/abs/1308.2099>

## Related publications, not included in the thesis

- E** O. Embréus, S. Newton, A. Stahl, E. Hirvijoki, and T. Fülöp, *Numerical calculation of ion runaway distributions*. Submitted to Physics of Plasmas. <http://arxiv.org/abs/1502.06739>
- F** G.I. Pokol, A. Kómár, A. Budai, A. Stahl, and T. Fülöp, *Quasi-linear analysis of the extraordinary electron wave destabilized by runaway electrons*, Physics of Plasmas **21**, 102503 (2014). <http://dx.doi.org/10.1063/1.4895513> <http://arxiv.org/abs/1407.5788>
- G** A. Stahl, E. Hirvijoki, M. Landreman, J. Decker, G. Papp, and T. Fülöp, *Effective critical electric field for runaway electron generation*, Proceedings of 41th EPS Conference on Plasma Physics, Berlin, P2.049 (2014). <http://ocs.ciemat.es/EPS2014PAP/pdf/P2.049.pdf>
- H** A. Stahl, M. Landreman, T. Fülöp, G. Papp, and E. Hollmann, *Synchrotron radiation from runaway electron distributions in tokamaks*, Proceedings of 40th EPS Conference on Plasma Physics, Helsinki, P5.117 (2013). <http://ocs.ciemat.es/EPS2013PAP/pdf/P5.117.pdf>

# Contents

<b>Abstract</b>	<b>i</b>
<b>Publications</b>	<b>iii</b>
<b>1 Introduction</b>	<b>1</b>
<b>2 Runaway electrons</b>	<b>3</b>
2.1 Runaway generation mechanisms . . . . .	4
2.2 Critical electric field and critical momentum . . . . .	5
2.3 Dreicer field . . . . .	6
2.4 Secondary runaway generation . . . . .	7
2.5 External circumstances – when is the necessary electric field generated? . . . . .	10
<b>3 Simulation of runaway electron momentum space dynamics</b>	<b>13</b>
3.1 Kinetic equation . . . . .	13
3.2 Collision operator and avalanche source term . . . . .	15
3.3 CODE – numerical scheme . . . . .	17
<b>4 Synchrotron radiation</b>	<b>19</b>
4.1 Single-particle synchrotron power spectrum . . . . .	20
4.2 Synchrotron power spectrum from a runaway distribution . . . . .	23
4.3 Radiation reaction force . . . . .	24
<b>5 Summary</b>	<b>29</b>
<b>Bibliography</b>	<b>31</b>
<b>Included papers (A-D)</b>	<b>37</b>



# Acknowledgments

It is a pleasure to acknowledge the neverending encouragement and support of my supervisor, Professor Tünde Fülöp, without whom I would have likely been forever stuck in a black hole. Her ambition and high standards continue to take her to new academic heights, and her enthusiasm tends to drag her colleagues along. I'm lucky to call myself one of them.

Thanks also to my co-supervisors Matt Landreman and István Pusztai. Matt, ever the wizard, laid the foundation for a lot of the work in this thesis, and I have benefited greatly from his insight and attention to detail. István, intelligent and with a sharp eye, yet the most helpful and humble of men, has made an important contribution in the later stages with his experience and somewhat fresh view of the subject.

The day “at the office” would certainly be less interesting without the company of Albert, Geri, Eero and Ola. Input on any topic imaginable can be expected from this Swiss Army knife of a group. I'm fortunate to share my days with you. Thanks especially to Geri for teaching me the meaning of flawless, and to Eero and Ola for going to the heart of the matter.

Finally; to Hedvig. Thank you for being more convinced than I am, which means the world, and for putting up with quirks and cookies. You are the joy and music.



# 1 Introduction

In plasma physics, many interesting phenomena occur that are outside our everyday experience. One of these is the generation of so-called *runaway electrons* (or simply *runaways*) – electrons that under certain conditions get continuously accelerated by electric fields [1, 2]. The dynamics of the process are such that the runaways quickly reach relativistic energies; they move with speeds very close to that of light. Runaways appear in a variety of atmospheric and astrophysical contexts, as discussed in Sec. 2.5. Apart from their intrinsic interest, these highly energetic particles are also a cause for concern in the context of fusion reactors [3].

Generating electric power using controlled thermonuclear fusion reactions is a promising concept for a future sustainable energy source [4, 5, 6], but stable and controllable operating conditions are required for a successful fusion power plant. The presence of runaway electrons in the plasmas of fusion reactors under certain circumstances is one of the main remaining hurdles on the road to realization of fusion power production [7], as the runaways carry with them the potential to severely damage the machine when they get transported out of the plasma and strike the wall [8]. There is therefore a great need to improve the understanding of the mechanisms that generate and suppress runaway electrons, and to better describe their dynamics.

The runaway electrons are created in the middle of a plasma with a temperature in excess of 1 million Kelvin, and there is no way to measure or diagnose them in situ. One way to further the understanding about the relevant processes is to instead look at the radiation generated by the runaways. Of particular interest is the synchrotron radiation the runaways emit as a consequence of their spiraling motion around the field lines of the strong magnetic field used to confine the plasma in the fusion reactor. Synchrotron emission represents a unique tool, as it provides information about the runaway population in the middle of the plasma, and not only once the runaways have escaped confinement and are lost to the wall (as is the case with for instance hard x-ray emission [9]).

In this thesis, the dynamics of runaway electrons are studied using a new efficient numerical tool (CODE, described in Chapter 3). Runaway acceleration is only possible if the electric field in the plasma exceeds a certain value [10], and special attention is given to properties of the runaways in cases where the field is close to this critical field. The spectrum of the synchrotron radiation emitted by the runaways is also studied in detail, as well as the back-reaction on the runaway population associated with its emission.

We begin by a general introduction to the runaway electron phenomenon.

## 2 Runaway electrons

In short, a *runaway electron* is an electron in a plasma which experiences a net accelerating force during a sustained time – enough to give it a significantly larger momentum than the thermal electron population. How to categorize runaways is not always clear, and the use of this slightly vague definition is discussed in Sec. 4.3.

The accelerating force on the electron is supplied by an induced electric field  $\mathbf{E}$ , so that  $\mathbf{F}_E = -e\mathbf{E}$ , where  $e$  is the elementary charge. Meanwhile, Coulomb interaction with the other particles in the plasma (commonly denoted *collisions*) introduces a friction force  $\mathbf{F}_C(v)$ . The origin of the runaway phenomenon is that  $\mathbf{F}_{C,\parallel}$ , the component of the friction force parallel to the magnetic (and electric) fields, is a non-monotonic function of the particle velocity, with a maximum around the electron thermal speed ( $v_{\text{th}}$ ), see Fig. 2.1. Therefore  $\partial\mathbf{F}_{C,\parallel}/\partial v < 0$  for particles that are faster than  $v_{\text{th}}$  – the friction force on these particles *decreases* with increasing particle velocity. The physical origin of this effect is that the faster particles spend less time in the vicinity of other particles in the plasma; the impulse delivered to the fast particle in each encounter decreases as the particle speed increases. This implies that if the accelerating force is sufficiently strong to overcome the friction at the current velocity  $v_0$  of the particle,  $|\mathbf{F}_E| > \mathbf{F}_{C,\parallel}(v_0)$ , it will be able to accelerate the particle for all  $v > v_0$ , i.e. the particle will get continuously accelerated to relativistic energies as long as the electric field persists.

The picture is complicated by the fact that apart from Coulomb collisions, several other forces can contribute to the dynamics, in particular radiation reaction forces associated with synchrotron and bremsstrahlung emission. In these cases, the force balance is altered, ultimately preventing the electrons from reaching arbitrarily high momenta. Radiation reaction due to synchrotron emission is studied in Paper B and discussed in Sec. 4.3, and its effect on the runaway distribution is investigated in Paper C.

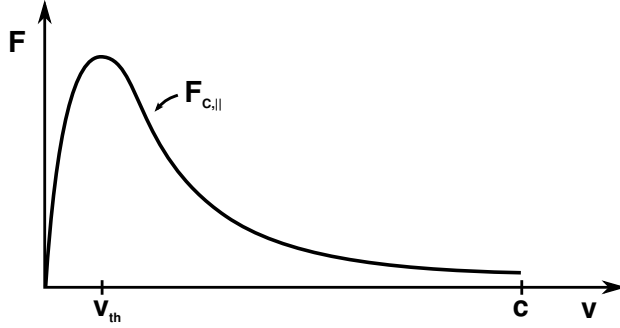


**Figure 2.1:** Friction force on an electron due to collisions, as a function of its velocity (schematic).

## 2.1 Runaway generation mechanisms

There are two main mechanisms for generating runaways, referred to as *Dreicer* [1, 2] and *avalanche* [11, 12, 13] generation. In the former, initially thermal electrons become runaways by a gradual diffusion through momentum space until they reach a velocity where they may run away. Once some runaways exist, they may impart a large fraction of their momentum to a thermal electron in a single event, known as a knock-on collision. This generates a second runaway if both electrons still belong to the runaway region after the collision. This process is also called *secondary* runaway generation, as it requires the presence of a *primary* runaway seed, and leads to an exponential growth of the runaway population (hence the name avalanche).

Primary runaways can also be produced by processes other than momentum space diffusion, for instance by highly energetic  $\gamma$ -rays through pair production, or in tritium decay (in fusion plasmas). There is a fourth primary runaway mechanism – *hot-tail generation* [14, 15] – which relies on a rapid cooling of the plasma. If the plasma cooling time scale is significantly shorter than the collision time at which particles equilibrate, electrons that initially constituted the high-energy part of the bulk distribution can form a drawn-out tail. If a strong electric field is also present, some of these tail electrons may belong to the runaway-region of momentum space and will therefore get accelerated. Under certain circumstances, hot-tail generation can be the dominating runaway generation mechanism – albeit for a short time – and may provide a strong seed for multiplication by the avalanche mechanism. Of the primary

runaway processes, only Dreicer generation will be considered in this thesis, and we will occasionally use *primary* interchangeably with *Dreicer* (as is often informally done).

Let us examine the two main mechanisms in greater detail, starting with the general criteria for runaway growth.

## 2.2 Critical electric field and critical momentum

The *critical electric field* for runaway electron generation,  $E_c$ , is the weakest field at which runaway is possible, see Fig. 2.2. The accelerating force due to  $E_c$  is simply equal (and opposite) to the sum of all the friction forces acting to slow the particle down, at the speed  $v_{\min}$  where they are minimized:  $-e\mathbf{E}_c = -\min(\sum_i \mathbf{F}_{f,i}(v)) = -\sum_i \mathbf{F}_{f,i}(v_{\min})$ . In the simplest case, the only friction force is due to collisions with electrons (due to the mass difference, the energy lost by the electrons in collisions with ions is neglected, as are all other forces):  $eE_c = F_{ee,\parallel}(v = v_{\min})$ . In this case, it is easy to obtain an expression for  $E_c$ . The (arbitrary speed) friction force is given by [16]

$$F_{ee,\parallel}(v) = \frac{1 + \gamma}{\gamma v^2} m_e c^3 \nu_{\text{rel}} = \frac{1 + \gamma}{\gamma v^2} \frac{n_e e^4 \ln \Lambda}{4\pi \varepsilon_0^2 m_e}, \quad (2.1)$$

where  $v$  is the speed of the particle,  $\gamma = 1/\sqrt{1 - v^2/c^2}$ ,  $m_e$  is the electron rest mass,  $c$  is the speed of light,  $n_e$  is the number density of electrons,  $\ln \Lambda$  is the Coulomb logarithm (see for instance Refs. [16, 17]),  $\varepsilon_0$  is the vacuum permittivity and

$$\nu_{\text{rel}} = \frac{n_e e^4 \ln \Lambda}{4\pi \varepsilon_0^2 m_e^2 c^3} \quad (2.2)$$

is the *collision frequency* for a highly relativistic particle. The collision frequency is defined such that  $1/\nu$  is the average time for a particle to experience a  $90^\circ$  deflection due to an accumulation of small-angle Coulomb interactions (which are much more frequent than large-angle collisions in fusion plasmas).

Apart from the trivial solution at  $v = 0$ , the friction force in Eq. 2.1 is minimized as  $v \rightarrow c$  (we have already mentioned that  $F_{ee,\parallel}$  is monotonically decreasing for large velocities). We thus have that the critical field is  $E_c = \frac{1}{e} F_{ee,\parallel}(v \rightarrow c)$  or

$$E_c = \frac{n_e e^3 \ln \Lambda}{4\pi \varepsilon_0^2 m_e c^2}, \quad (2.3)$$

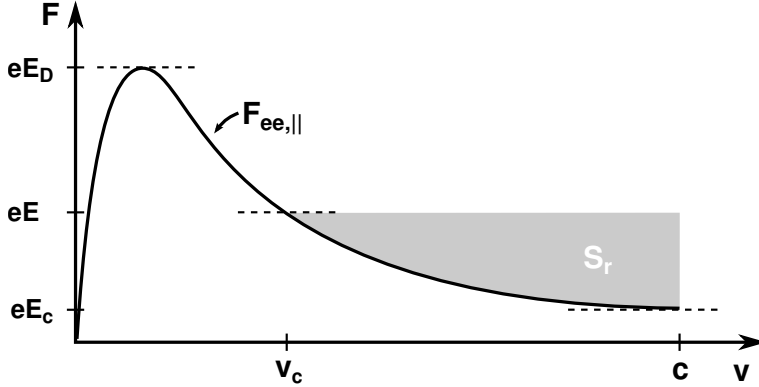


**Figure 2.2:** Forces corresponding to collisional friction against electrons ( $F_{ee,\parallel}$ ), the critical field ( $E_c$ ) and the Dreicer field ( $E_D$ ). The runaway region in momentum space ( $S_r$ ) associated with the electric field  $E$  is also shown.

which was first obtained by Connor and Hastie in 1975 [10].

For any  $E > E_c$ , there exists some speed  $v_c$  above which the electric field overcomes the friction force. Particles with a velocity greater than this *critical speed* will run away, and  $v_c$  thus marks the lower boundary of the *runaway region*  $S_r$  in velocity space. This is illustrated in Fig. 2.2. It is customary to study runaways in terms of momentum rather than velocity. The *critical momentum* is a simple function of the electric field strength if expressed in terms of the relativistic mass factor  $\gamma$  or the normalized momentum  $p = \gamma v/c$ ,

$$\gamma_c = \sqrt{\frac{E/E_c}{E/E_c - 1}}, \quad p_c = \frac{1}{\sqrt{E/E_c - 1}} \quad (2.4)$$

(if the electron is assumed to move parallel to the magnetic field lines).

## 2.3 Dreicer field

The critical field  $E_c$  corresponds to the field balancing the minimum of the collisional friction force. The *Dreicer field*,  $E_D$  [1, 2], on the other hand, balances the maximum of the friction force, which is located around  $v = v_{th}$ , with

$v_{\text{th}} = \sqrt{2T_e/m_e}$  the electron thermal speed and  $T_e$  is the electron temperature<sup>1</sup>. For  $E \gtrsim E_D$ , the accelerating force can overcome the friction at all particle velocities, and the whole electron population can thus run away. The critical and Dreicer fields are related by the ratio of the thermal energy to the electron rest mass-energy:

$$E_D = \frac{m_e c^2}{T_e} E_c = \frac{n_e e^3 \ln \Lambda}{4\pi \epsilon_0^2 T_e}. \quad (2.5)$$

In practice, the electric field is almost always much smaller than the Dreicer field.

Due to momentum space transport processes, new particles steadily diffuse into the runaway region, increasing the runaway density. The growth rate of the runaway population due to Dreicer generation [10, 18, 19, 20] is described by

$$\frac{dn_r}{dt} = C n_e \nu_{ee} \epsilon^{-3(1+Z_{\text{eff}})/16} \exp\left(-\frac{1}{4\epsilon} - \sqrt{\frac{1+Z_{\text{eff}}}{\epsilon}}\right), \quad (2.6)$$

where  $\epsilon = E/E_D$ ,  $n_r$  is the runaway number density,

$$\nu_{ee} = \frac{n_e e^4 \ln \Lambda}{4\pi \epsilon_0^2 m_e^2 v_{\text{th}}^3} \quad (2.7)$$

is the collision frequency,  $C$  is an undetermined constant of order unity [3], and  $Z_{\text{eff}}$  is the effective ion charge, which is a measure of the plasma composition ( $Z_{\text{eff}} = 1$  is a plasma consisting of pure hydrogen, or otherwise singly charged ions). Note that the growth rate depends on (and is exponentially small in)  $E/E_D$ , not  $E/E_c$ . This means that even if the field is significantly larger than  $E_c$ , the runaway production rate may be very small if  $E \ll E_D$ . The importance of this effect, which is in essence a temperature dependence, is discussed and quantified in Paper B. The runaway growth rate as a function of  $E/E_D$  is plotted in Fig. 2.3.

## 2.4 Secondary runaway generation

Secondary runaways are formed as already existing runaways collide with thermal electrons, if the collision imparts enough momentum to the thermal electron to kick it into the runaway region while the incoming (primary) electron

<sup>1</sup>It is customary in plasma physics to let  $T_e \equiv k_B T_e$ , so that the ‘‘temperature’’ actually is the thermal energy, and to express it in eV.

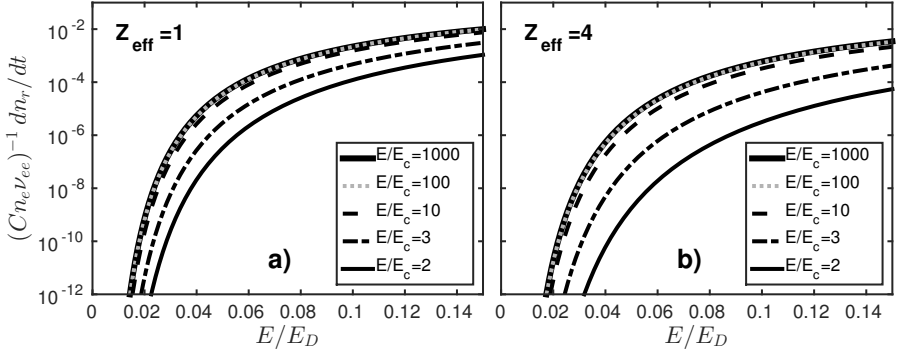


**Figure 2.3:** Normalized primary runaway growth rate as a function of normalized electric field strength. Physically, the different curves correspond to different temperatures (large  $E/E_c$  denotes the low-temperature limit). A comparison of panels a) and b) shows that the presence of high- $Z$  ions (impurities) significantly reduces the runaway growth rate. Note also the sharp cutoff at low  $E/E_D$  for all values of  $E/E_c$ .

still remains a runaway itself. Such events are referred to as *close* or *knock-on* collisions. To be able to contribute to the avalanche process, an incoming runaway must thus have a momentum  $p > 2p_c$ .

The avalanche growth rate was first calculated by Rosenbluth & Putvinski [13], who also derived an approximate operator for avalanche generation (see Sec. 3.1). In a cylindrical plasma, the growth rate takes the form

$$\frac{dn_r}{dt} \simeq n_r \nu_{\text{rel}} \frac{(\mathcal{E} - 1)}{c_z \ln \Lambda} \left( 1 - \mathcal{E}^{-1} + \frac{4(Z_{\text{eff}} + 1)^2}{c_z^2(\mathcal{E}^2 + 3)} \right)^{-1/2}, \quad (2.8)$$

where  $\mathcal{E} = E/E_c$  and  $c_z = \sqrt{3(Z_{\text{eff}} + 5)/\pi}$ . In the limit where  $E \gg E_c$  and  $Z_{\text{eff}} = 1$ , this simplifies to

$$\frac{dn_r}{dt} \simeq \sqrt{\frac{\pi}{2}} n_r \nu_{\text{rel}} \frac{(\mathcal{E} - 1)}{3 \ln \Lambda}. \quad (2.9)$$

The growth rate is proportional to the runaway density  $n_r$ , meaning that the growth is exponential (hence the name avalanche). We also note that the dependence on  $E$  is linear in Eq. (2.9), and nearly so in the more general expression (2.8), whereas it is exponential in Eq. (2.6) for the primary growth

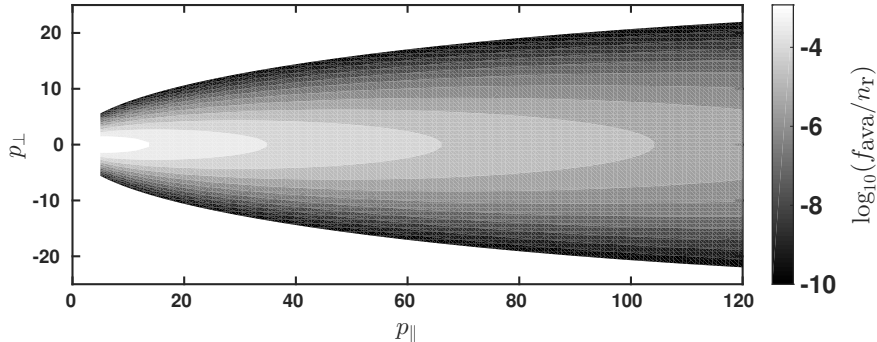


**Figure 2.4:** Contour plot of the analytical avalanche distribution function in Eq. (2.10) for  $T_e = 1$  keV,  $n_e = 1 \cdot 10^{20} \text{ m}^{-3}$ ,  $Z_{\text{eff}} = 1.5$  and  $E/E_c = 15$ . The distribution is not valid for the bulk plasma, and is therefore cut off at low momentum (in this case at  $p_{\parallel} = 5$ ).

rate. Therefore, avalanche generation tends to dominate for weak fields (as long as there is some runaway population to start with), but for strong fields primary generation becomes more important.

Assuming secondary generation dominates, the quasi-steady-state runaway distribution function (see Sec. 3.1) can be calculated analytically [21], and is given by

$$f_{\text{ava}}(p_{\parallel}, p_{\perp}) = \frac{n_r \hat{E}}{2\pi c_z p_{\parallel} \ln \Lambda} \exp\left(-\frac{p_{\parallel}}{c_z \ln \Lambda} - \frac{\hat{E} p_{\perp}^2}{2p_{\parallel}}\right), \quad (2.10)$$

where  $\hat{E} = (E/E_c - 1)/(1 + Z_{\text{eff}})$ , and  $p_{\parallel}$  and  $p_{\perp}$  are the parallel (to the magnetic field) and perpendicular components of the normalized particle momentum. Equation (2.10) is valid when  $\gamma \gg 1$  and  $E/E_c \gg 1$ . An example distribution is plotted in Fig. 2.4 – it is distinctly beam-like in appearance. The distribution in Eq. (2.10) was used extensively in the calculation of synchrotron spectra in Paper C, and also as a benchmark in Paper A.

## 2.5 External circumstances – when is the necessary electric field generated?

In order for runaways to be generated, a comparatively long-lived electric field is required. Due to the natural tendency of the plasma to screen out such fields, they are not normally present. However in certain situations, for instance if a current running through the plasma changes quickly, an electric field is induced which may be sufficient to lead to runaway formation. Runaway electrons do form in atmospheric plasmas – they have been linked to for instance lightning discharges [22], impulsive radio emissions [23], and terrestrial gamma-ray flashes [24] – and in the mesosphere [25]. In astrophysical plasmas, they are expected to form in for instance solar flares [26] and large-scale filamentary structures in the galactic center [27]. Under certain circumstances, also other plasma species may run away. Both ion and positron runaway have been investigated in recent work (see Refs. [28, 29, 30], as well as Paper E). Our main interest in this thesis is however electron runaway in the context of magnetic confinement thermonuclear fusion.

During start-up of the most common type of fusion device, the *tokamak* [31], a plasma is formed by the ionization of a gas. For this, a strong electric field is usually needed. Runaways may form in this situation, however their formation can usually be avoided by maintaining a high enough gas density. The case of a changing current is more problematic. In a tokamak, a strong current is driven through the plasma in order to generate the necessary confining magnetic geometry. Very abrupt changes in plasma current occur during so-called *disruptions* – large catastrophic events in which the plasma becomes unstable, cools down, and eventually terminates [7, 32]. As the plasma cools, the resistivity increases drastically, and a large electric field is induced which tries to maintain the current. Near the magnetic axis of the tokamak, this field is often strong enough to lead to runaway generation, and runaway beams in the center of the plasma have been observed during disruptions in many tokamaks. Runaways can also be generated in so-called sawtooth crashes [33], and even during normal stable operation if the density is low enough (the accelerating field in this case is due to the “loop voltage” which maintains the plasma current). Some plasma heating schemes produces an elevated tail in the electron velocity distribution, and can lead to increased runaway production, should a disruption occur [34].

The main reason for the interest in runaway research is that the runaways pose a serious threat to tokamak devices. During disruptions, a large portion of the

## 2.5 External circumstances – when is the necessary electric field generated?

initial plasma current (which can be several megaampere) can be converted into runaway current, but the runaways eventually become so energetic that they are not well confined by the magnetic fields. Unless their generation is successfully mitigated, the runaways eventually escape the plasma and hit the wall where they can destroy sensitive components or degrade the wall material.

In present day tokamaks, runaways are a nuisance, but usually not a serious threat. The avalanche multiplication of a primary runaway seed is predicted to scale exponentially [13] with plasma current, however, and it is believed that in future devices (such as ITER [35] and eventually commercial fusion reactors), which will have a larger current, the problem will be much more severe. In these devices, disruptions can essentially not be tolerated at all, and much effort is devoted to research on runaway and disruption mitigation techniques (see for instance Refs. [36, 37]).



# 3 Simulation of runaway electron momentum space dynamics

Although the single particle estimates considered in Chapter 2 can be useful in understanding some of the phenomena associated with runaways, a complete and thorough understanding of their dynamics can only be gained through treating the full kinetic problem. Although in some idealized situations, the equations can be solved analytically, in general the interplay between the various processes involved in the momentum-space transport of electrons must be studied using numerical tools.

Previously, the code ARENA [38], which uses Monte Carlo methods to model momentum-space diffusion, has successfully been employed for this task, however in this case the Monte Carlo approach is not competitive when it comes to the use of computational resources. In terms of fully kinetic continuum codes, two comprehensive tools with extensive capabilities exist in LUKE [39, 40, 41] and CQL3D [14, 42]. Both of these are however multipurpose tools with much functionality which is not necessarily important to the runaway problem.

In Paper A, a new lightweight and efficient tool for calculating runaway dynamics is developed. It is called CODE (COLLisional Distribution of Electrons), and is a kinetic continuum code constructed specifically with the runaway problem in mind. It solves the kinetic equation, including electric field and collisions, in 2D momentum space in a uniform plasma (no magnetic field curvature or plasma parameter gradients). In this section, we will look at the formulation of the problem and how it is solved in CODE.

## 3.1 Kinetic equation

When it comes to describing plasma phenomena, several theoretical frameworks of varying degrees of complexity (and explanatory power), have been

developed. Fluid theories, although tractable, numerically efficient, and useful in other contexts, are based on the assumption that the plasma particles are everywhere thermally distributed, and can be described by Maxwellian distributions. In order to describe the runaway electron phenomenon, such a model is inadequate, as the runaways by definition constitute a high-energy (non-thermal) tail of the particle distribution. It is therefore necessary to resort to the use of *kinetic theory*, where the distribution of particle positions and velocities is the prime object of study.

The so-called *kinetic equation* describes the evolution of a distribution of plasma particles of species  $a$ ,  $f_a(\mathbf{x}, \mathbf{p}, t)$ , according to

$$\frac{\partial f_a}{\partial t} + \frac{\partial}{\partial \mathbf{x}} (\dot{\mathbf{x}} f_a) + \frac{\partial}{\partial \mathbf{p}} (\dot{\mathbf{p}} f_a) = C_a \{f_a\} + S, \quad (3.1)$$

where  $\mathbf{x}$  and  $\mathbf{p}$  denote the position and momentum, respectively, and  $\dot{\mathbf{p}}$  describes the macroscopic equations of motion (given for instance by the Lorentz-force due to the presence of macroscopic electric and magnetic fields). The *collision operator*  $C_a$  describes microscopic interactions between the plasma particles (collisions), which are normally treated separately from the macroscopic interactions.  $S$  represents any sources or sinks of particles, such as ionization and recombination of neutral atoms or fueling in laboratory plasmas. Under certain conditions, the collisions can be neglected, in which case Eq. (3.1) (with  $S = 0$ ) is known as the *Vlasov equation*. With a generally valid collision operator, it is the *Boltzmann equation*, although in practice several assumptions must be made to be able to treat the collisions. When only two-particle interactions are considered, and it is assumed that the momentum transfer in each collision is very small, the Boltzmann collision operator simplifies to the Fokker-Planck collision operator, and Eq. (3.1) is correspondingly called the *Fokker-Planck equation* [43]. This operator is sufficient to treat primary runaway generation, but is not able to describe the knock-on avalanche process in which the momentum transfer to the secondary particle is significant. Avalanche generation is instead treated by including a special source term  $S_{\text{ava}}$ , detailed in Sec. 3.2.

In general, the distribution  $f_a$  is a six-dimensional quantity and is very demanding to treat in its entirety. Various approximations are routinely employed to reduce the kinetic equation to a manageable number of dimensions (see for instance Ref. [16]). When studying runaway formation, the momentum space dynamics is the prime interest, and for many purposes, the plasma can be assumed to be spatially homogeneous. In addition, one of the

momentum-space dimensions (describing the rapid gyro-motion around the magnetic field lines) can be averaged over if a sufficiently strong magnetic field is present (so that the gyro-radius is ignorable in comparison to the typical length scale of the gradients in the plasma and the gyration time is short compared to the time scales of other processes). CODE therefore solves the kinetic equation in two momentum-space dimensions only, which allows for fast calculation while retaining most of the relevant physics. The assumption of spatial homogeneity is the most severe one, especially in systems such as fusion devices where magnetic field curvature is non-negligible in practice. LUKE and CQL3D both retain a radial dependence (as they were developed specifically for modeling tokamak plasmas), which allows for the study of for instance electron trapping effects on runaway dynamics [44]. Nevertheless, close to the tokamak magnetic axis (where the majority of runaway electrons are formed), the assumption of spatial homogeneity is well justified.

The two momentum-space dimensions are conveniently described by the coordinates  $(p, \xi)$ , where  $p = \gamma v/c$  is the normalized momentum and  $\xi = p_{\parallel}/p$  is the cosine of the particle pitch angle (which characterizes the pitch of the helix that describes the particle orbit around a magnetic field line). In these coordinates, the kinetic equation can be expressed as

$$\frac{\partial f_e}{\partial t} - \underbrace{\frac{eE_{\parallel}}{m_e c} \left( \xi \frac{\partial f_e}{\partial p} + \frac{1 - \xi^2}{p} \frac{\partial f_e}{\partial \xi} \right)}_{\text{electric field}} + \underbrace{\frac{\partial}{\partial \mathbf{p}} \cdot (\mathbf{F}_{\text{rad}} f_e)}_{\text{radiation reaction}} = C_e \{f_e\} + S_{\text{ava}}, \quad (3.2)$$

where the second term describes the acceleration due to the electric field and the third term describes the effects of synchrotron emission back-reaction (see Sec. 4.3 and Eq. 4.12). In CODE, this equation is solved for the electron distribution. CODE can calculate the time evolution of  $f_e$ , starting from some initial (usually Maxwellian) distribution, but can also determine the (quasi) steady-state distribution directly in the absence of sources.

## 3.2 Collision operator and avalanche source term

Accurate treatment of runaway electron dynamics requires a fully relativistic formulation of the equations. A generally valid momentum-conserving Fokker-Planck collision operator exists [45, 46], but its use would complicate the numerical implementation substantially. CODE instead employs a collision operator derived in Ref. [47] using asymptotic matching between the

highly relativistic operator in Ref. [48] (derived from the operator in Ref. [45] in the limit of a non-relativistic Maxwellian background plasma) and the corresponding well-known non-relativistic operator (see for instance [16]). The collision operator in Ref. [47] is valid for arbitrary energies, but consists of only the so-called test-particle part of the full operator (describing collisions between the distribution  $f$  and a background Maxwellian population of electrons). It is therefore not momentum-conserving. This approximation is justified in the case of runaway studies, since momentum-conservation has a significant effect on the plasma bulk (influencing for instance the conductivity), but is much less important in the tail of the distribution. Collisions with ions are modeled such that they only contribute to pitch-angle scattering of the electrons; the energy transfer in the collisions is neglected due to the mass difference between the particle species.

The collision operator is:

$$C_e\{f\} = \frac{1}{p^2} \frac{\partial}{\partial p} p^2 \left[ C_A \frac{\partial f}{\partial p} + C_F f \right] + \frac{C_B}{p^2} \frac{\partial}{\partial \xi} (1 - \xi^2) \frac{\partial f}{\partial \xi}, \quad (3.3)$$

where

$$\begin{aligned} C_A &= \frac{\Gamma}{v} \Psi(x), \\ C_B &= \frac{\Gamma}{2v} \left[ Z_{\text{eff}} + \phi(x) - \Psi(x) + \frac{\delta^4 x^2}{2} \right], \\ C_F &= \frac{\Gamma}{T_e} \Psi(x), \end{aligned} \quad (3.4)$$

$\delta = v_{\text{th}}/c$ ,  $x = v/v_{\text{th}}$ ,  $\phi$  is the error function,  $\Psi = (2x^2)^{-1} [\phi - x \text{d}\phi/\text{d}x]$  is the Chandrasekhar function and  $\Gamma = 4\pi n_e e^4 \ln \Lambda$ .

The knock-on collisions are modeled using an operator derived by Rosenbluth and Putvinski [13]. It assumes that the incoming primary electron has infinite momentum, and therefore experiences no momentum loss in the knock-on collision. Due to this assumption and the kinematics of the problem, the source is a  $\delta$ -function in  $\xi$  – secondary particles are generated only along a specific curve in momentum space, corresponding to  $\xi = \xi_2 \equiv p/(1 + \sqrt{1 + p^2})$ . This is illustrated in Fig. 3.1. The source is given by

$$S_{\text{RP}}(p, \xi) = \frac{n_r \nu_{\text{rel}}}{4\pi \ln \Lambda} \delta(\xi - \xi_2) \frac{1}{p^2} \frac{\partial}{\partial p} \left( \frac{1}{1 - \sqrt{1 + p^2}} \right). \quad (3.5)$$

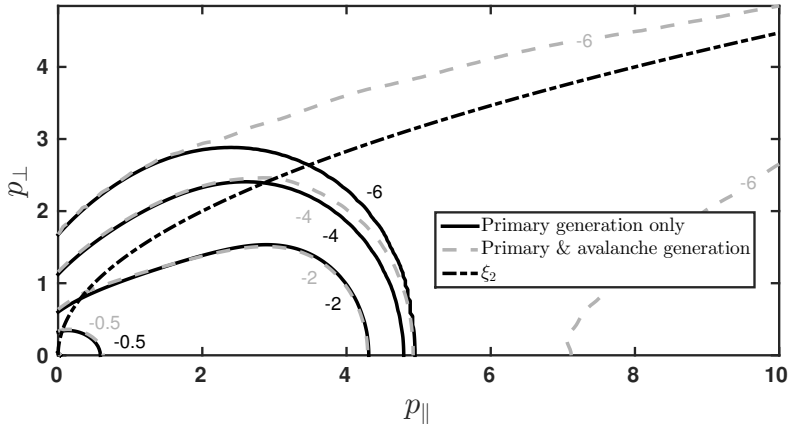


**Figure 3.1:** Contour plots of electron distributions with only primary runaway generation (black, solid) and with both primary and avalanche generation (gray, dashed) calculated using CODE. The plotted quantity is  $\log_{10}(f/n_r)$ . The avalanche source in Eq. (3.5) generates runaways along  $\xi = \xi_2$ , which leads to an increased particle density close to  $\xi_2$ , compared to the case with only primary generation. The feature is easily seen at high momentum, and is smeared out due to momentum-space transport processes.

The Rosenbluth-Putvinski source is proportional to the runaway density, and thus leads to exponential growth, as intended. It does however assume that all runaways move with the speed of light (or equivalently have infinite momentum). This means that it tends to overestimate the magnitude of the source, especially at high energies (in reality there are very few primary runaways that have enough energy to generate a secondary runaway with high energy). A less approximate avalanche source can be derived based on the Møller cross-section for electron-electron scattering [49, 50]. Such a source is implemented in CQL3D [14, 42].

### 3.3 CODE – numerical scheme

The main purpose of CODE is to be a fast and efficient numerical tool for studying the runaway electron distribution function. The numerical method

was chosen with this in mind, and is a significant improvement over some of the existing tools. In particular, in the absence of the secondary runaway source, the quasi-steady-state (time-asymptotic) electron distribution can be calculated with the inversion of a single matrix, which makes the computation extremely fast.

The two momentum-space dimensions  $(p, \xi)$  in CODE are treated differently – the momentum is discretized using fourth order finite differences, whereas the pitch-angle coordinate is spectrally decomposed into Legendre polynomials  $P_l(\xi)$ . The distribution function at momentum-space coordinates  $(p_n, \xi)$  is then represented by the sum

$$f(p_n, \xi) = \sum_{l=0}^{l_{\max}} f_l(p_n) P_l(\xi). \quad (3.6)$$

The Legendre polynomials have favorable properties for formulating the kinetic equation as a system of linear equations which can be solved using efficient standard matrix inversion techniques. Although faster results could surely be obtained using a lower-level language, CODE is written in Matlab to take advantage of the ease of use and the excellent matrix-handling capabilities of that language. For a detailed description of the numerical implementation, see Paper A.

The finite-difference discretization in  $p$  allows for the use of non-uniform momentum grids. As the momentum difference between the plasma bulk and the far runaway tail can be very large, this is a very useful feature as it allows for the use of the necessary high resolution close to the bulk but at the same time makes it possible to cover an extensive momentum range without using a prohibitively large amount of grid points.

In Paper A, distributions from CODE are compared to the analytical avalanche distribution in Eq. (2.10) with excellent agreement in the region of mutual applicability, and CODE runaway growth rates are also found to agree perfectly with an early numerical study [51]. For the work related to Papers B and C, CODE was extended via the inclusion of a term describing synchrotron radiation back-reaction (see Sec. 4.3).

In terms of speed, CODE was compared to ARENA on the same computer hardware, and showed an improvement in computation time of roughly 7 orders of magnitude for the same level of convergence!

## 4 Synchrotron radiation

Charged particles in accelerated motion emit radiation [52]. In the presence of a magnetic field, the particles in a plasma follow helical orbits as a consequence of the Lorentz force. In other words, they are continuously accelerated “inwards” – perpendicular to their velocities. The radiation emitted by electrons due to this motion is known as *cyclotron radiation* if the particle is non-relativistic (or mildly so) and *synchrotron radiation* if it is highly relativistic (the names come from the types of devices where the radiation was first observed [53]). Synchrotron radiation has many applications in the study of samples in condensed matter physics, materials science, biology and medicine, where it is used in for instance scattering and diffraction studies, and for spectroscopy and tomography [54]. The radiation is usually produced using dedicated facilities (synchrotrons), but is also emitted in some natural processes, in particular in astrophysical contexts, where it can be used as a diagnostic tool.

From the distinction between cyclotron and synchrotron radiation, it is evident that in a non-relativistic plasma (with a temperature significantly below 511 keV), only the far tail of the electron distribution may emit synchrotron radiation. The only plasma particles that reach highly relativistic energies are the runaway electrons. The study of the synchrotron emission from a plasma is thus a very important source of information about the runaways, and their dynamics.

The theory of synchrotron radiation was first derived by Schott in 1912 [55], but was rediscovered, and to a large extent reworked, by Schwinger in the 40’s [56]. In the rest frame of the particle, the synchrotron radiation is emitted almost isotropically, however the transformation to the lab frame introduces a strong forward beaming effect, see Fig. 4.1. Since the motion of the particle is predominantly parallel to the magnetic field lines (the runaways are assumed to be accelerated by  $E_{\parallel}$ ), the synchrotron radiation will be emitted in this direction as well, even though it is their perpendicular motion that is the cause of the emission. The (half) opening angle of the synchrotron beam is given by  $\alpha \simeq 1/\gamma$  [56], and can thus in principle serve as an estimate

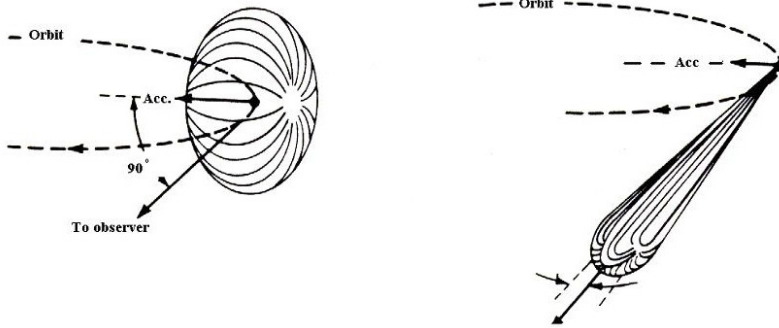


**Figure 4.1:** The shape of the emitted radiation in the case of cyclotron (left, low energy) and synchrotron (right, highly relativistic) emission, respectively. After R. Bartolini/Wikimedia Commons/Public Domain.

for the energy of the emitting particle. Since the synchrotron radiation is directed, its observation requires detectors in the right location and with the right field of view. In many tokamak experiments this necessitates the use of dedicated cameras for the study of synchrotron emission from runaways, and the number of such set-ups around the world is limited. Detailed discussions of the properties of synchrotron radiation can be found in Refs. [54, 57, 52]. Some recent images of runaway synchrotron emission in tokamaks are given in Refs. [58, 59].

## 4.1 Single-particle synchrotron power spectrum

The frequency of the cyclotron or synchrotron radiation emitted by a particle is a multiple of the frequency with which it orbits the magnetic field line (the *cyclotron frequency* or *gyro frequency*). In the case of cyclotron emission, the fundamental and the first few harmonics dominate completely, whereas for the high energy synchrotron emission, the high harmonics (up to some cut off) are dominant. Since these are spaced very close together, synchrotron radiation essentially has a continuous frequency spectrum [57]. The emission can span a large part of the electromagnetic spectrum, from microwaves to hard x rays, depending on the frequency of the gyro-motion.

In terms of quantities convenient for plasma physics [57], the synchrotron

power spectrum can be expressed as

$$\mathcal{P}(\lambda) = \frac{1}{\sqrt{3}} \frac{ce^2}{\varepsilon_0 \lambda^3 \gamma^2} \int_{\lambda_c/\lambda}^{\infty} K_{5/3}(l) dl, \quad (4.1)$$

where  $K_\nu(x)$  is the modified Bessel function of the second kind of order  $\nu$ , and  $\lambda_c$  is a critical wavelength given by

$$\lambda_c = \frac{4\pi}{3} \frac{c}{\omega_c \gamma^2} = \frac{4\pi}{3} \frac{cm_e \gamma_{\parallel}}{eB \gamma^2}, \quad (4.2)$$

with  $\omega_c$  the cyclotron frequency,  $\gamma_{\parallel} = (1 - v_{\parallel}^2/c^2)^{-1/2}$  and  $B$  the magnetic field strength. The spectrum is plotted in Fig. 4.2 for a few different parameter sets. There is a sharp cutoff at short wavelengths, but a much slower decay towards longer wavelengths. In the conditions found in tokamak plasmas, the synchrotron spectrum primarily peaks for micrometer (near-infrared) wavelengths, although for highly energetic runaway beams, emission in the visible part of the electromagnetic spectrum is also observed.

## In a toroidal magnetic field

Equation 4.1 considers the radiation emitted due to pure gyro-motion around a straight field-line. In a tokamak, particle orbits are more complicated since both the motion around the torus, that due to the helicity of the field lines, and various drifts contribute. The synchrotron power spectrum for a particle trajectory including the gyro motion, the motion along a toroidal magnetic field, and vertical centrifugal drift was derived by I. M. Pankratov in 1999 [60], and is

$$\mathcal{P}(\lambda) = \frac{ce^2}{\varepsilon_0 \lambda^3 \gamma^2} \left\{ \int_0^{\infty} g(y) J_0(a\xi y^3) \sin(h(y)) dy - 4a \int_0^{\infty} y J'_0(a\xi y^3) \cos(h(y)) dy - \frac{\pi}{2} \right\}, \quad (4.3)$$

where  $a = \eta/1 + \eta^2$ ,  $g(y) = y^{-1} + 2y$ ,  $h(y) = 3\xi (y + y^3/3) / 2$ ,

$$\xi = \frac{4\pi}{3} \frac{R}{\lambda \gamma^3 \sqrt{1 + \eta^2}}, \quad (4.4)$$

$$\eta = \frac{eBR v_{\perp}}{\gamma m_e v_{\parallel}^2} \simeq \frac{\omega_c R v_{\perp}}{\gamma c v_{\parallel}}, \quad (4.5)$$

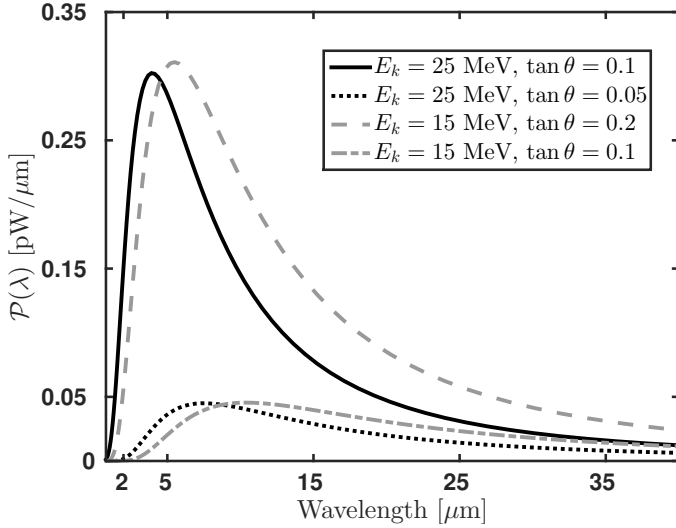


**Figure 4.2:** Synchrotron power spectrum for a single electron with kinetic energy  $E_k$  and pitch described by  $\tan \theta = v_{\perp}/v_{\parallel}$  (with  $\theta$  the pitch angle). Note that both the peak wavelength and the emitted power are sensitive to both the particle energy and pitch. In particular, it is possible to produce similar synchrotron spectra using significantly different parameter sets (see also Sec. 4.2).

$R$  is the tokamak major radius,  $J_{\nu}(x)$  is the Bessel function, and  $J'_{\nu}(x)$  its derivative with respect to the argument. The integrands in Eq. (4.3) are products of Bessel functions and trigonometric functions, and are highly oscillatory with respect to the variable of integration ( $y$ ). Because of this, numerical integration – although possible – is not straight-forward. The derivation in Ref. [60] assumes that the frequency of the radiation is much larger than the electron cyclotron frequency,  $\omega \gg \omega_c$  (which is normally the case in tokamak plasmas [60]). The calculation is also restricted to only consider highly relativistic electrons ( $p \gg 1$ ) with  $p_{\parallel} \gg p_{\perp}$ . Large aspect ratio is also assumed, so that the results are valid close to the magnetic axis of a tokamak.

In Ref. [60], two asymptotic forms of Eq. (4.3) are also derived. These use approximations for the integrals, meaning that they are more suited for numerical implementation. In Paper D, the three formulas of Ref. [60], together with Eq. (4.1), are studied and compared for a variety of tokamak parameters

and it is concluded that the cylindrical limit (Eq. 4.1) is a good approximation to Eq. (4.3) in large devices, whereas in devices with small major radius, one of the asymptotic expressions is more suitable in terms of approximating Eq. (4.3). In general, however, the power spectra are similar.

## 4.2 Synchrotron power spectrum from a runaway distribution

The total synchrotron power emitted by an electron in circular motion is [56]

$$P_{\text{tot}} = \frac{e^2}{6\pi\epsilon_0} \frac{\omega_0}{\rho} \beta_{\perp}^3 \gamma^4, \quad (4.6)$$

where  $\omega_0$  is the angular velocity,  $\rho$  is the radius of curvature and  $\beta_{\perp} = v_{\perp}/c$ . In a magnetized plasma, the angular velocity and curvature radius are the Larmor frequency and radius, respectively,  $\omega_c = eB/\gamma m_e$  and  $r_L = v_{\perp}/\omega_c$ . This gives

$$P_{\text{tot}} = \frac{e^2}{6\pi\epsilon_0} \frac{\omega_c^2}{v_{\perp}} \beta_{\perp}^3 \gamma^4 = \frac{e^4}{6\pi\epsilon_0 m_e^2 c} B^2 \beta_{\perp}^2 \gamma^2 = \frac{e^4}{6\pi\epsilon_0 m_e^2 c} B^2 p_{\perp}^2. \quad (4.7)$$

The total emitted power thus scales as  $p_{\perp}^2 = \gamma^2 (v_{\perp}/c)^2 \simeq \gamma^2 (v_{\perp}/v_{\parallel})^2 = \gamma^2 \tan^2 \theta \approx \gamma^2 \theta^2$ , with  $\theta$  the particle pitch angle, meaning that the most energetic particles with the largest pitch angles emit most strongly. It has therefore been assumed that the emission from these particles completely dominate the spectrum, and when interpreting synchrotron spectra and emission patterns the simplification of considering a mono-energetic beam of electrons with a single pitch has frequently been employed [58, 61, 62, 63].

Less approximate synchrotron spectra can be calculated by using the average emission from the entire runaway distribution, according to

$$P(\lambda) = \frac{2\pi}{n_r} \int_{S_r} f_r(p, \xi) \mathcal{P}(p, \xi, \lambda) p^2 dp d\xi, \quad (4.8)$$

where  $f_r$  is the runaway distribution function,  $\mathcal{P}$  is one of the single particle emission formulas (i.e. Eqs. 4.1 and 4.3), and  $S_r$  is the runaway region in momentum space. A numerical tool for efficiently performing this type of calculation, SYRUP (SYnchrotron spectra from RUNaway Particles), was developed in connection with Paper D, and the resulting spectra are studied

in detail in the paper. The assumption of a mono-energetic runaway beam is examined, and found to be very poor in many cases (in terms of agreement with the spectrum from the entire runaway population), qualitatively as well as quantitatively. Including the full runaway distribution in the calculation is thus absolutely necessary to obtain accurate results, and in this sense SYRUP constitutes a significant improvement over previous methods. The synchrotron spectrum is very sensitive to changes in the plasma parameters and electric field strength, something which can not be captured by the mono-energetic approximation. This sensitivity is due to the dependence on the exact shape of the runaway distribution. The sensitivity to certain changes typical of kinetic instabilities driven by runaways was also studied (in Paper D, as well as in Paper F).

In the analysis in Paper D, analytical runaway distributions were used. The analytical formula (Eq. 2.10) represents a steady-state limit, however, and is not able to capture dynamical effects or describe the synchrotron emission in the early stages of the runaway population evolution. In Paper A, numerical distributions from CODE were used to study both dynamic phenomena and distributions where the avalanche mechanism was not dominant. Excellent agreement was also found between the numerical distribution and Eq. (2.10) at sufficiently late times.

### 4.3 Radiation reaction force

As an electron emits a photon, it receives an impulse in the opposite direction due to the conservation of momentum. There is therefore a *radiation reaction force*  $F_{\text{rad}}$  associated with the emission of synchrotron radiation, the parallel component of which acts as an additional effective friction on the electrons, in addition to that due to collisions. Synchrotron emission only becomes important at relativistic energies, however, and contrary to collisional friction, the radiation reaction force increases with particle speed, in accordance with the estimate in the previous section. This completely changes the parallel force balance for runaways at high momentum, as depicted in Fig. 4.3. Note that, although in the following discussion it is convenient to consider only the parallel force balance of single particles, in reality the problem involves transport processes in two-dimensional momentum space and must in general be treated using numerical tools, as discussed in Chapter 3.

Two effects in particular are of interest in Fig. 4.3. Firstly, the friction due

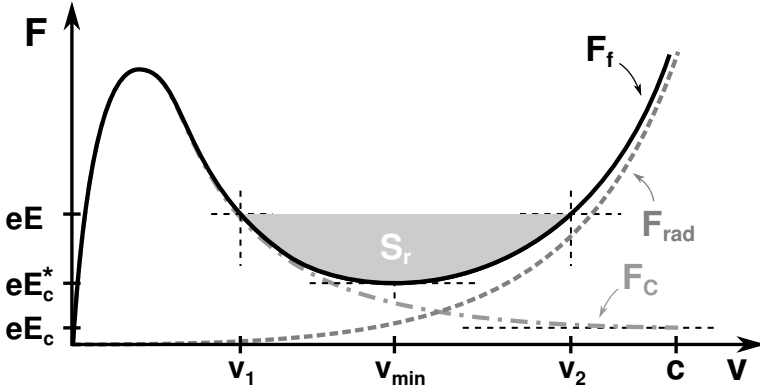


**Figure 4.3:** Forces associated with total friction ( $F_f$ ), collisional friction ( $F_C$ ), synchrotron radiation reaction ( $F_{\text{rad}}$ ), the (classical) critical field ( $E_c$ ) and the critical field including synchrotron radiation reaction ( $E_c^*$ ). The two critical velocities  $v_1$  and  $v_2$  corresponding to the electric field  $E$  are also shown, together with the runaway region ( $S_r$ ), and the speed at which the total friction force is minimized ( $v_{\text{min}}$ ). C.f Fig. 2.2. Note that the velocity scale is chosen for clarity – in practice both  $v_{\text{min}}$  and  $v_2$  lie close to  $c$ .

to radiation emission effectively prevents runaways from reaching arbitrary energies; for a given electric field  $E$  there are two speeds ( $v_1$  and  $v_2$ ) for which the total friction force equals the accelerating force:  $F_f(v_{1,2}) = |eE|$ . Runaway is only possible for  $v_1 < v < v_2$ . Radiation back-reaction associated with both synchrotron and bremsstrahlung emission has been considered previously as a possible mechanism limiting the achievable runaway energy [12, 64].

Secondly, the minimum of the friction force is no longer found at  $v = c$  (see Sec. 2.2), but at some intermediate speed  $v_{\text{min}}$  (which is still close to  $c$ ) satisfying  $v_1 < v_{\text{min}} < v_2$ . Crucially, the minimum field necessary for runaway generation to occur – the critical field – is raised accordingly:

$$|eE_c^*| = F_f(v_{\text{min}}), \quad (4.9)$$

where  $E_c^*$  is the critical field in the presence of radiation reaction forces and  $E_c^* > E_c$ , as depicted in Fig. 4.3. The importance of this and other effects related to the critical field are examined in Paper B.

The introduction of an upper bound to the runaway region prompts us to

reexamine what constitutes a runaway. Although formally, electrons with  $v > v_2$  are not experiencing runaway acceleration, particles with speeds around  $v_2$  will always be well separated from the bulk, and will therefore be a part of the high-energy tail of the distribution (in fact they are likely to be the most energetic particles of all). In addition, should they lose energy due to transport processes, they would become runaways again, and thus get accelerated anew. Pragmatically, a case can therefore be made for retaining the old definition of the runaway region ( $S_R : p > p_c$ ).

In dynamic situations, a related issue is encountered. If the electric field drops below the critical field  $E_c^*$  after a substantial runaway tail has been generated, a large population of fast particles is still present (and will remain so for some time due to its low collisionality). These particles are potentially hazardous, despite the fact that no “runaway region” exists.

An additional consequence of the existence of an upper bound to the runaway region is that particles tend to accumulate in the vicinity of the speed  $v_2$  in velocity space. Provided certain conditions are satisfied, this process can even lead to the formation of a non-monotonic feature – a “bump” – on the runaway tail, as illustrated in Fig. 4.4. This effect is investigated analytically in Paper C, and the results confirmed through a comparison with CODE calculations. The distributions exhibiting this non-monotonic feature are true steady-state solutions to the kinetic equation, unlike the case of a “conventional” runaway tail which represents a quasi-steady state since there is a continuous flow of particles from the thermal population into the runaway region and to ever higher energies. In a true steady-state, the argument can be made that the concept of electron runaway is no longer appropriate, since no net acceleration occurs. Still, the particles that make up the non-monotonic feature have speeds significantly larger than the bulk population, and this in principle divides the distribution into a thermal bulk and a fast particle beam. Again, the fast particles may cause damage to the machine, even though they are not formally runaways.

The issues discussed here highlight that what constitutes a runaway is no longer clear-cut (or even necessarily the relevant parameter to consider) when several effective friction forces or dynamical processes are taken into account.

## Operator for synchrotron radiation reaction

To understand the full role of radiation reaction effects on plasma dynamics, the single particle treatment considered above is insufficient. Fully kinetic sim-

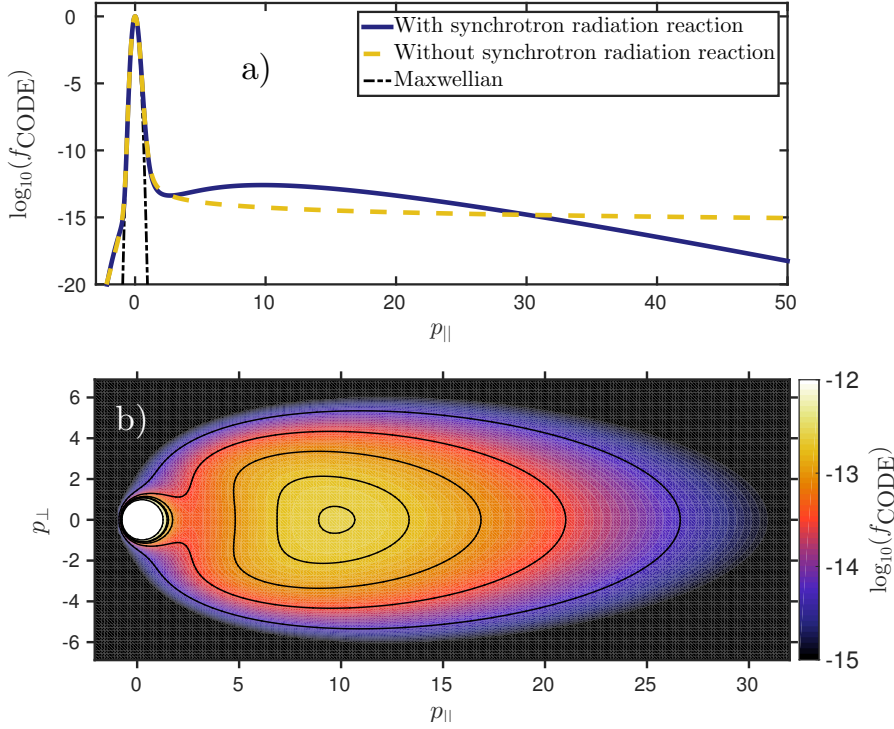


**Figure 4.4:** Steady-state electron distribution function calculated using CODE in the absence of avalanche generation. In a), the distribution for  $p_{\perp} = 0$  is shown, with and without synchrotron radiation reaction included. In b), momentum-space contours of the distribution with radiation reaction included are shown. The plotted quantity is the base 10 logarithm of the normalized distribution in CODE (see Paper A for details). The parameters  $T_e = 5$  keV,  $n_e = 2 \cdot 10^{19} \text{ m}^{-3}$ ,  $Z_{\text{eff}} = 1.2$ ,  $E/E_c = 2$ , and  $B = 2.5$  T where used. In this case, the “bump” is located around  $p_{\parallel} = 10$ , which corresponds to a kinetic energy of 4.6 MeV.

ulations are necessary to capture the interplay between the various processes affecting the momentum-space transport. Such calculations can be performed using CODE, but for this application an operator describing the radiation reaction is needed.

The radiation reaction can be calculated from the Abraham-Lorentz-Dirac force affecting a charged particle [65],

$$\mathbf{F}_{\text{rad}} = \frac{q^2 \gamma^2}{6\pi\epsilon_0 c^3} \left[ \ddot{\mathbf{v}} + \frac{3\gamma^2}{c^2} (\mathbf{v} \cdot \dot{\mathbf{v}}) \dot{\mathbf{v}} + \frac{\gamma^2}{c^2} \left( \mathbf{v} \cdot \ddot{\mathbf{v}} + \frac{3\gamma^2}{c^2} (\mathbf{v} \cdot \dot{\mathbf{v}})^2 \right) \mathbf{v} \right],$$

where  $q$  is the charge and  $\mathbf{v}$  the velocity of the particle. Assuming that the magnetic force dominates, so that the particle is only accelerated perpendicular to its velocity ( $\mathbf{v} \cdot \dot{\mathbf{v}} = 0$ ), the expression simplifies to

$$F_{\text{rad},p} = -\frac{\gamma p (1 - \xi^2)}{\tau_r} \quad (4.10)$$

$$F_{\text{rad},\xi} = -\frac{p\xi\sqrt{1 - \xi^2}}{\gamma\tau_r}, \quad (4.11)$$

where  $\tau_r = q^4 B^2 / 6\pi\epsilon_0 (m_e c)^3$  is the radiation damping time scale. The radiation reaction force enters the kinetic equation, Eq. (3.2), as an operator on the form  $(\partial/\partial\mathbf{p}) \cdot (\mathbf{F}_{\text{rad}} f_e)$ , and using Eqs. (4.10) and (4.11), the explicit form is

$$\frac{\partial}{\partial\mathbf{p}} \cdot (\mathbf{F}_{\text{rad}} f_e) = \frac{1 - \xi^2}{\gamma\tau_r} \left( - \left[ \frac{2}{(1 - \xi^2)} + 4p^2 \right] f_e - \gamma^2 p \frac{\partial f_e}{\partial p} + \xi \frac{\partial f_e}{\partial \xi} \right). \quad (4.12)$$

The force acts to limit both the particle energy and pitch, which is to be expected as the emitted synchrotron power is proportional to  $P_{\text{tot}} \sim \gamma^2 \theta^2$  (see Sec. 4.2). Equations (4.10) and (4.11) were derived in Ref. [64], the first paper to properly consider the role of radiation reaction in runaway dynamics, but in that paper a high energy limit was used which lead to an incorrect (or rather incomplete) expression in place of Eq. (4.12), as pointed out in [66].

## 5 Summary

The runaway phenomenon is a fascinating one; friction that decreases with speed is outside our everyday experience. Still, since the vast majority of the matter in the universe is in a plasma state, runaway electrons appear in many astrophysical contexts, as well as in atmospheric phenomena here on Earth.

The work described in this thesis has focused on runaway electrons in the context of magnetic confinement thermonuclear fusion devices, since for this application the runaways are of particular interest because of their destructive potential. The ability to avoid substantial runaway formation – or achieve controlled mitigation of runaway beams, should they form – is of utmost importance in future fusion devices such as ITER. To facilitate the establishment of operational limits and the development of control and mitigation systems, increased theoretical understanding of runaway dynamics, together with improved techniques for diagnosing the runaway population in experiments, is needed. The work presented here has implications in both these areas.

In Paper A, CODE, an efficient numerical tool for studying the electron distribution function in 2-D momentum space in the presence of electric fields and collisions, is developed. It allows for detailed study of both steady-state and dynamical properties of runaway electron populations. CODE is then used in Paper B to investigate factors that influence the critical electric field for runaway generation (Eq. 2.3), and is extended to include an operator for synchrotron radiation back-reaction (Eq. 4.12). It is shown that the temperature of the plasma strongly influences the normalized effective field  $E/E_c$  needed for significant runaway production, and that the inclusion of synchrotron radiation-reaction effects can reduce the runaway growth rate strongly for weak electric fields, leading to a de-facto increase in the critical field. Recent experimental observations, in which the critical field in the tokamak DIII-D was determined to be a factor 3–5 higher than  $E_c$  [67], are also examined, and it is found that the apparent increase in the critical field can for the most part be attributed to shortcomings of the method used to assess the runaway growth.

Paper C examines the steady-state runaway distribution function analytically in the presence of synchrotron radiation-reaction, and describes the formation of a non-monotonic feature on the distribution tail. Analytical estimates for the location of this feature in momentum space, as well as criteria for its formation, are derived and validated through comparison with CODE calculations. Such a feature could give rise to a bump-on-tail instability, which would lead to dissipation of the runaways, and can thus potentially greatly influence the runaways dynamics.

The synchrotron radiation emitted by relativistic particles in a magnetized plasma is an important source of information, as it provides information in situ about several properties of the otherwise inaccessible runaways. The emitted synchrotron spectrum is studied in detail in Paper D using analytical distributions of steady-state avalanche-dominated runaway populations, and in Paper A using CODE distributions. The use of numerical distributions in this context allows for analysis of the time evolution of the synchrotron spectrum. The work has important implications for the interpretation of experimental synchrotron spectra, as it is shown that a commonly used assumption – that the synchrotron spectrum is completely dominated by the emission from the most strongly emitting runaway electrons – can be highly inaccurate. The sensitivity of the spectrum to the background plasma parameters and perturbations to the electron distribution are also highlighted, and various formulas describing the single-particle synchrotron emission spectrum are examined.

Although parameter values relevant for fusion plasmas have been used throughout this work, the results in Papers A–C are generally applicable since no effects specific to fusion plasmas (such as a toroidal magnetic field geometry) have been included. In parts of Paper D, the focus on tokamaks is more pronounced, as various expressions accurately describing synchrotron emission in toroidal plasmas specifically, are investigated.

# Bibliography

- [1] H. Dreicer, Electron and ion runaway in a fully ionized gas I, *Phys. Rev.* **115**, 238 (1959), DOI: 10.1103/PhysRev.115.238.
- [2] H. Dreicer, Electron and ion runaway in a fully ionized gas II, *Phys. Rev.* **117**, 329 (1960), DOI: 10.1103/PhysRev.117.329.
- [3] P. Helander, L.-G. Eriksson, and F. Andersson, Runaway acceleration during magnetic reconnection in tokamaks, *Plasma Physics and Controlled Fusion* **44**, B247 (2002), DOI: 10.1088/0741-3335/44/12B/318.
- [4] W. J. Nuttall, Fusion as an energy source: Challenges and opportunities, Tech. Rep. (Institute of Physics Report, 2008) [http://www.iop.org/publications/iop/2008/file\\_38224.pdf](http://www.iop.org/publications/iop/2008/file_38224.pdf).
- [5] F. F. Chen, *An Indispensable Truth - How Fusion Power Can Save the Planet* (Springer, 2011).
- [6] J. P. Freidberg, *Plasma Physics And Fusion Energy* (Cambridge University Press, 2007).
- [7] T. Hender, J. Wesley, J. Bialek, A. Bondeson, A. Boozer, R. Buttery, A. Garofalo, T. Goodman, R. Granetz, Y. Gribov, O. Gruber, M. Gryaznevich, G. Giruzzi, S. Günter, N. Hayashi, P. Helander, C. Hegna, D. Howell, D. Humphreys, G. Huysmans, A. Hyatt, A. Isayama, S. Jardin, Y. Kawano, A. Kellman, C. Kessel, H. Koslowski, R. L. Haye, E. Lazzaro, Y. Liu, V. Lukash, J. Manickam, S. Medvedev, V. Mertens, S. Mirnov, Y. Nakamura, G. Navratil, M. Okabayashi, T. Ozeki, R. Paccagnella, G. Pautasso, F. Porcelli, V. Pustovitov, V. Riccardo, M. Sato, O. Sauter, M. Schaffer, M. Shimada, P. Sonato, E. Strait, M. Sugihara, M. Takechi, A. Turnbull, E. Westerhof, D. Whyte, R. Yoshino, H. Zohm, and the ITPA MHD, Disruption and Magnetic Control Topical Group, Chapter 3: MHD stability, operational limits and disruptions, *Nuclear Fusion* **47**, S128 (2007), DOI: 10.1088/0029-5515/47/6/S03.

- 
- [8] E. Hollmann, G. Arnoux, N. Commaux, N. Eidietis, T. Evans, R. Granetz, A. Huber, D. Humphreys, V. Izzo, A. James, T. Jernigan, M. Lehnen, G. Maddaluno, R. Paccagnella, P. Parks, V. Philipps, M. Reinke, D. Rudakov, F. Saint-Laurent, V. Sizyuk, E. Strait, J. Wesley, C. Wong, and J. Yu, Plasma-surface interactions during tokamak disruptions and rapid shutdowns, *Journal of Nuclear Materials* **415**, S27 (2011), DOI: 10.1016/j.jnucmat.2010.10.009, Proceedings of the 19th International Conference on Plasma-Surface Interactions in Controlled Fusion.
- [9] A. James, M. Austin, N. Commaux, N. Eidietis, T. Evans, E. Hollmann, D. Humphreys, A. Hyatt, V. Izzo, T. Jernigan, R. L. Haye, P. Parks, E. Strait, G. Tynan, J. Wesley, and J. Yu, Measurements of hard x-ray emission from runaway electrons in DIII-D, *Nuclear Fusion* **52**, 013007 (2012), DOI: 10.1088/0029-5515/52/1/013007.
- [10] J. Connor and R. Hastie, Relativistic limitations on runaway electrons, *Nuclear Fusion* **15**, 415 (1975), DOI: 10.1088/0029-5515/15/3/007.
- [11] Y. A. Sokolov, "Multiplication" of accelerated electrons in a tokamak, *JETP Letters* **29**, 218 (1979).
- [12] R. Jayakumar, H. Fleischmann, and S. Zweben, Collisional avalanche exponentiation of runaway electrons in electrified plasmas, *Physics Letters A* **172**, 447 (1993), DOI: 10.1016/0375-9601(93)90237-T.
- [13] M. Rosenbluth and S. Putvinski, Theory for avalanche of runaway electrons in tokamaks, *Nuclear Fusion* **37**, 1355 (1997), DOI: 10.1088/0029-5515/37/10/I03.
- [14] S. Chiu, M. Rosenbluth, R. Harvey, and V. Chan, Fokker-planck simulations mylb of knock-on electron runaway avalanche and bursts in tokamaks, *Nuclear Fusion* **38**, 1711 (1998), DOI: 10.1088/0029-5515/38/11/309.
- [15] P. Helander, H. Smith, T. Fülöp, and L.-G. Eriksson, Electron kinetics in a cooling plasma, *Physics of Plasmas* **11**, 5704 (2004), DOI: 10.1063/1.1812759.
- [16] P. Helander and D. J. Sigmar, *Collisional Transport in Magnetized Plasmas* (Cambridge University Press, 2002).
- [17] F. F. Chen, *Introduction to plasma physics and controlled fusion*, 2nd ed., Vol. 1 (Plenum Press, 1984).

- [18] A. V. Gurevich, On the theory of runaway electrons, *Sov. Phys. JETP* **12**, 904 (1961).
- [19] M. D. Kruskal and I. B. Bernstein, PPPL report MATT-Q-20, p. 174, (1962).
- [20] R. H. Cohen, Runaway electrons in an impure plasma, *Physics of Fluids* (1958-1988) **19**, 239 (1976), DOI: 10.1063/1.861451.
- [21] T. Fülöp, G. Pokol, P. Helander, and M. Lisak, Destabilization of magnetosonic-whistler waves by a relativistic runaway beam, *Physics of Plasmas* **13**, 062506 (2006), DOI: 10.1063/1.2208327.
- [22] A. Gurevich, G. Milikh, and R. Roussel-Dupre, Nonuniform runaway air-breakdown, *Physics Letters A* **187**, 197 (1994), DOI: 10.1016/0375-9601(94)90062-0.
- [23] H. E. Tierney, R. A. Roussel-Dupré, E. M. D. Symbalisty, and W. H. Beasley, Radio frequency emissions from a runaway electron avalanche model compared with intense, transient signals from thunderstorms, *Journal of Geophysical Research* **110** (2005), DOI: 10.1029/2004JD005381.
- [24] U. S. Inan and N. G. Lehtinen, Production of terrestrial gamma-ray flashes by an electromagnetic pulse from a lightning return stroke, *Geophysical Research Letters* **32** (2005), DOI: 10.1029/2005GL023702.
- [25] T. F. Bell, V. P. Pasko, and U. S. Inan, Runaway electrons as a source of red sprites in the mesosphere, *Geophysical Research Letters* **22**, 2127 (1995), DOI: 10.1029/95GL02239.
- [26] G. D. Holman, Acceleration of runaway electrons and Joule heating in solar flares, *Astrophysical Journal* **293**, 584 (1985).
- [27] H. Lesch and W. Reich, The origin of monoenergetic electrons in the arc of the galactic center – particle acceleration by magnetic reconnection, *Astronomy and Astrophysics* **264**, 493 (1992).
- [28] T. Fülöp and M. Landreman, Ion runaway in lightning discharges, *Phys. Rev. Lett.* **111**, 015006 (2013), DOI: 10.1103/PhysRevLett.111.015006.
- [29] T. Fülöp and S. Newton, Alfvénic instabilities driven by runaways in fusion plasmas, *Physics of Plasmas* **21**, 080702 (2014), DOI: 10.1063/1.4894098.
- [30] T. Fülöp and G. Papp, Runaway positrons in fusion plasmas, *Phys. Rev. Lett.* **108**, 225003 (2012), DOI: 10.1103/PhysRevLett.108.225003.

- [31] J. Wesson, *Tokamaks*, 2nd ed. (Oxford Science Publications, 1997).
- [32] J. Wesson, R. Gill, M. Hugon, F. Schüller, J. Snipes, D. Ward, D. Bartlett, D. Campbell, P. Duperrex, A. Edwards, R. Granetz, N. Gottardi, T. Hender, E. Lazzaro, P. Lomas, N. L. Cardozo, K. Mast, M. Nave, N. Salmon, P. Smeulders, P. Thomas, B. Tubbing, M. Turner, and A. Weller, Disruptions in JET, *Nuclear Fusion* **29**, 641 (1989), DOI: 10.1088/0029-5515/29/4/009.
- [33] C. Barnes and J. Strachan, Sawtooth oscillations in the flux of runaway electrons to the PLT limiter, *Nuclear Fusion* **22**, 1090 (1982), DOI: 10.1088/0029-5515/22/8/010.
- [34] J. R. Martín-Solís, B. Esposito, R. Sánchez, F. M. Poli, and L. Panaccione, Enhanced production of runaway electrons during a disruptive termination of discharges heated with lower hybrid power in the Frascati Tokamak Upgrade, *Phys. Rev. Lett.* **97**, 165002 (2006), DOI: 10.1103/PhysRevLett.97.165002.
- [35] <http://www.iter.org>.
- [36] E. Hollmann, M. Austin, J. Boedo, N. Brooks, N. Commaux, N. Eidietis, D. Humphreys, V. Izzo, A. James, T. Jernigan, A. Loarte, J. Martin-Solis, R. Moyer, J. Muñoz-Burgos, P. Parks, D. Rudakov, E. Strait, C. Tsui, M. V. Zeeland, J. Wesley, and J. Yu, Control and dissipation of runaway electron beams created during rapid shutdown experiments in DIII-D, *Nuclear Fusion* **53**, 083004 (2013), DOI: 10.1088/0029-5515/53/8/083004.
- [37] E. M. Hollmann, P. B. Aleynikov, T. Fülöp, D. A. Humphreys, V. A. Izzo, M. Lehnen, V. E. Lukash, G. Papp, G. Pautasso, F. Saint-Laurent, and J. A. Snipes, Status of research toward the ITER disruption mitigation system, *Physics of Plasmas* **22**, 021802 (2015), DOI: 10.1063/1.4901251.
- [38] L.-G. Eriksson and P. Helander, Simulation of runaway electrons during tokamak disruptions, *Computer Physics Communications* **154**, 175 (2003), DOI: 10.1016/S0010-4655(03)00293-5.
- [39] Y. Peysson, J. Decker, and R. W. Harvey, Advanced 3-D electron fokker-planck transport calculations, *AIP Conference Proceedings* **694**, 495 (2003), DOI: 10.1063/1.1638086.
- [40] J. Decker and Y. Peysson, DKE: A fast numerical solver for the 3D drift kinetic equation, *Tech. Rep. EUR-CEA-FC-1736* (Euratom-CEA, 2004).
- [41] Y. Peysson and J. Decker, Calculation of rf current drive in tokamaks, *AIP Conference Proceedings* **1069**, 176 (2008), DOI: 10.1063/1.3033701.

- [42] R. W. Harvey, V. S. Chan, S. C. Chiu, T. E. Evans, M. N. Rosenbluth, and D. G. Whyte, Runaway electron production in DIII-D killer pellet experiments, calculated with the CQL3D/KPRAD model, *Physics of Plasmas* **7**, 4590 (2000), DOI: 10.1063/1.1312816.
- [43] M. N. Rosenbluth, W. M. MacDonald, and D. L. Judd, Fokker-planck equation for an inverse-square force, *Phys. Rev.* **107**, 1 (1957), DOI: 10.1103/PhysRev.107.1.
- [44] E. Nilsson, J. Decker, Y. Peysson, E. Hollmann, and F. Saint-Laurent, Kinetic modelling of runaway electron avalanches in tokamak plasmas, *Proceedings of the 41st EPS Conference on Plasma Physics* **O2.303** (2014).
- [45] S. T. Beliaev and G. I. Budker, *Sov. Phys. Dokl.* **1**, 218 (1956).
- [46] B. J. Braams and C. F. F. Karney, Conductivity of a relativistic plasma, *Physics of Fluids B: Plasma Physics* **1**, 1355 (1989), DOI: 10.1063/1.858966.
- [47] G. Papp, M. Drevlak, T. Fülöp, and P. Helander, Runaway electron drift orbits in magnetostatic perturbed fields, *Nuclear Fusion* **51**, 043004 (2011), DOI: 10.1088/0029-5515/51/4/043004.
- [48] P. Sandquist, S. E. Sharapov, P. Helander, and M. Lisak, Relativistic electron distribution function of a plasma in a near-critical electric field, *Physics of Plasmas* **13**, 72108 (2006), DOI: 10.1063/1.2219428.
- [49] C. Möller, *Annalen der Physik* **14**, 531 (1932).
- [50] W. Heitler, *The Quantum Theory of Radiation*, 3rd ed. (Dover, 1954).
- [51] R. M. Kulsrud, Y.-C. Sun, N. K. Winsor, and H. A. Fallon, Runaway electrons in a plasma, *Phys. Rev. Lett.* **31**, 690 (1973), DOI: 10.1103/PhysRevLett.31.690.
- [52] J. D. Jackson, *Classical Electrodynamics*, 3rd ed. (Wiley & Sons, 1999).
- [53] F. R. Elder, A. M. Gurewitsch, R. V. Langmuir, and H. C. Pollock, Radiation from electrons in a synchrotron, *Phys. Rev.* **71**, 829 (1947), DOI: 10.1103/PhysRev.71.829.5.
- [54] E.-E. Koch, *Handbook on Synchrotron Radiation*, edited by E.-E. Koch, Vol. 1a (North Holland, 1983).
- [55] G. A. Schott, *Electromagnetic Radiation* (Cambridge University Press, 1912).

- 
- [56] J. Schwinger, On the classical radiation of accelerated electrons, *Phys. Rev.* **75**, 1912 (1949), DOI: 10.1103/PhysRev.75.1912.
- [57] G. Bekefi, *Radiation Processes in Plasmas*, edited by S. C. Brown (Wiley & Sons, 1966).
- [58] J. H. Yu, E. M. Hollmann, N. Commaux, N. W. Eidietis, D. A. Humphreys, A. N. James, T. C. Jernigan, and R. A. Moyer, Visible imaging and spectroscopy of disruption runaway electrons in DIII-D, *Physics of Plasmas* **20**, 042113 (2013), DOI: 10.1063/1.4801738.
- [59] R. J. Zhou, L. Q. Hu, E. Z. Li, M. Xu, G. Q. Zhong, L. Q. Xu, S. Y. Lin, J. Z. Zhang, and the EAST Team, Investigation of ring-like runaway electron beams in the EAST tokamak, *Plasma Phys. Control. Fusion* **55**, 055006 (2013), DOI: 10.1088/0741-3335/55/5/055006.
- [60] I. M. Pankratov, Analysis of the synchrotron radiation spectra of runaway electrons, *Plasma Physics Reports* **25**, 145 (1999).
- [61] R. Jaspers, N. J. L. Cardozo, A. J. H. Donné, H. L. M. Widdershoven, and K. H. Finken, A synchrotron radiation diagnostic to observe relativistic runaway electrons in a tokamak plasma, *Rev. Sci. Instrum.* **72**, 466 (2001), DOI: 10.1063/1.1318245.
- [62] I. M. Pankratov, Analysis of the synchrotron radiation emitted by runaway electrons, *Plasma Physics Reports* **22**, 535 (1996).
- [63] R. J. Zhou, I. M. Pankratov, L. Q. Hu, M. Xu, and J. H. Yang, Synchrotron radiation spectra and synchrotron radiation spot shape of runaway electrons in experimental advanced superconducting tokamak, *Physics of Plasmas* **21**, 063302 (2014), DOI: 10.1063/1.4881469.
- [64] F. Andersson, P. Helander, and L.-G. Eriksson, Damping of relativistic electron beams by synchrotron radiation, *Physics of Plasmas* **8**, 5221 (2001), DOI: 10.1063/1.1418242.
- [65] W. Pauli, *Theory of Relativity* (Dover, New York, 1981).
- [66] R. Hazeltine and S. Mahajan, Radiation reaction in fusion plasmas, *Physical Review E* **70**, 046407 (2004), DOI: 10.1103/PhysRevE.70.046407.
- [67] C. Paz-Soldan, N. W. Eidietis, R. Granetz, E. M. Hollmann, R. A. Moyer, J. C. Wesley, J. Zhang, M. E. Austin, N. A. Crocker, A. Wingen, and Y. Zhu, Growth and decay of runaway electrons above the critical electric field under quiescent conditions, *Physics of Plasmas* **21**, 022514 (2014), DOI: 10.1063/1.4866912.